Focusing a beam beyond the diffraction limit using a hyperlens-based device*

Zheng Guo-Xing(郑国兴)†, Zhang Rui-Ying(张瑞瑛), Li Song(李 松), He Ping-An(何平安), and Zhou Hui(周 辉)

School of Electronic Information, Wuhan University, Wuhan 430079, *China*

(Received 14 April 2011; revised manuscript received 23 June 2011)

A super-focusing device composed of a focusing objective and a hyperlens is proposed to focus an incident plane wave into the deep subwavelength dimension. In the device, the objective converts the incident plane wave into a convergent one. The half cylindrical hyperlens can support high wave vector k modes propagating towards its core. So the convergent wave can be focused into an ultrasmall spot beyond the diffraction limit. The layout is proposed for the super-focusing device and its characteristics are investigated theoretically. Numerical simulations verify that the focused beams are confined in a spot with a diameter of 16.3 nm in the focal plane of the focusing objective with a numerical aperture of 0.6, which corresponds to a super-resolution spot of $\lambda_0/23$ (λ_0 is the wavelength in vacuum). The simulations confirm the effectiveness of the proposed device.

Keywords: hyperlens, objective, super-focusing device, resolution

PACS: 78.67.Pt, 42.79.Bh, 42.25.Bs **DOI:** 10.1088/1674-1056/20/11/117802

1. Introduction

In the optical data storage area, a high numerical-aperture (NA) lens system is required to focus the collimated laser beam into a small spot for data recording and reading. The minimum dimension of the focused spot Δx in one direction, which is constrained by the equation $\Delta x \Delta k \approx 2\pi$[1] with Δk being the bandwidth of the angular spectrum, is determined by the maximum transverse wavenumber $k_{x,\max}$ ($\Delta k = 2k_{x,\max}$) in the focal plane. When the convergent wave with aperture angle θ propagates from the back surface to the focal plane of the lens, the largest transverse wavenumber in the focal plane is $k_0 \sin\theta$, where k_0 is the wavenumber in the vacuum, thus the minimum focused spot size is $\Delta x_{\min} = 2\pi/(2k_0 \sin\theta) = \lambda_0/(2\sin\theta)$, where λ_0 is the wavelength in the vacuum. To realize a smaller focused spot for high-density data storage, a suggested method is to place a solid immersion lens (SIL) with high refractive index in the proximity of the focal plane, which can narrow the focused spot size down to $\lambda_0/(2n\sin\theta) = \lambda_0/(2N_{\rm A})$, where n is the refractive index of the SIL material, and $N_{\rm A}$ is the numerical aperture. However, due to the limitation of the lens materials and the laser technology, it seems that techniques, which compress the beam size by means of decreasing wavelength and increasing numerical aperture, do not hold much potential for breakthrough in recent years. In fact, the key to overcoming the diffraction limit to obtain smaller beam spots lies in how to allow the convergent wave with its transverse wavenumber larger than k_0 to reach the focal plane without the amplitude decay. Based on this principle, in recent years, a lot of super-resolution imaging devices that consist of noble metals have been reported, such as the near-field superlens based on a silver slab,[2−7] the far-field superlens (FSL) combining a thin silver slab and sub-wavelength gratings,[1,8−11] and the ring-structured hyperlens.[12−17] However, none of those super-resolution imaging devices mentioned above can be used in the beam compressing directly. For example, the near-field planar superlens can only achieve a 1:1 imaging, and the far-field superlens can reconstruct an object only by numerical calculations based on the far-field spectrum information recorded by a charge-coupled device (CCD) camera[8,9] or by means of a complicated image-reconstructive setup.[10] Therefore, a more effective and simpler device is urgently needed for super-resolution focusing. The hy-

*Project supported by the National Natural Science Foundation of China (Grant No. 10904118), the Natural Science Foundation of Hubei Province, China (Grant No. 2009CDB211), and the Fundamental Research Funds for the Central Universities of China.

†Corresponding author. E-mail: gxzheng@whu.edu.cn

© 2011 Chinese Physical Society and IOP Publishing Ltd

perlens, which is capable of compressing and enlarging beams, brings a new way to us for sub-wavelength focusing. Featured by alternating metal and dielectric layers, the hyperlens is equivalent to a structured metamaterial with a positive tangential dielectric permittivity ε_θ and a negative radial dielectric permittivity ε_r. Meeting the hyperbolic dispersion relation[17] $k_r^2/\varepsilon_\theta + k_\theta^2/\varepsilon_r = k_0^2$ in the cylindrical coordinates, wave vectors k_r and k_θ can take unbounded values at a finite frequency. Such a desired lens can support not only high wave vector k modes (which decay away in the ordinary media) toward the core of the hyperlens, but also beam magnification or beam demagnification due to its cylindrical structure.

However, focusing the collimated beam requires that the aperture of the lens is large enough to envelope all incident beams. For the traditional hyperlens, a larger aperture requires more metal and dielectric layers, which will increase the difficulty in fabrication and reduce the system transmission. In this paper, we propose to use a focusing objective first to focus the incident beam and then place a hyperlens with a few layers near the focal plane of the objective to improve the resolution. Therefore, with the advantages of both high resolution and high transmission, the proposed hyperlens-based focusing device is a device with a simple design and a simple structure that can be used for the high-density near-field optical data storage and other potential applications requiring beam focusing.

The working principle and the characteristic analysis of the proposed device are presented first. Then the effectiveness of the device consisting of a microlens and a half cylindrical hyperlens is numerically demonstrated. The hyperlens is composed of alternating rings of silver (Ag) and aluminum oxide (Al_2O_3). Compared with the conventional focusing objective, our proposed device achieves a smaller focal spot with a dimension of 16.3 nm, corresponding to $\lambda_0/23$. The system transmission is calculated to be 5.3%, which is much higher than that of a single hyperlens ($\sim$0.1%) producing the same spot size. Finally, the influence of the innermost layer radius of the hyperlens on the focusing spot size and the system transmission is simulated and discussed.

2. Hyperlens-based focusing device

2.1. Working principle of the device

To illustrate the characteristics of the hyperlens, we present the dispersion relations of a conventional solid immersion lens and the hyperlens for comparison, as shown in Fig. 1. It can be seen that the wave vectors of the propagating waves in the solid immersion lens are localized within a circle of radius nk_0 and the evanescent wave featured by wavenumbers larger than nk_0 undergoes evanescent decay. The evanescent wave plays an important role in the solid immersion lens system[18] and is stimulated only in the interface when the conditions of the total internal reflection are met. Furthermore, the focusing objective with a high numerical aperture and the solid immersion lens made of a high refractive index material[19,20] are required. Nevertheless, the hyperlens is beyond such a limitation. In the hyperbolic lens, tangential wave vectors k_θ and radial wave vectors k_r satisfy a hyperbolic relation (shown in Fig. 1(b)), and thus the transmission of waves with tangential wave vectors larger than nk_0 is supported.

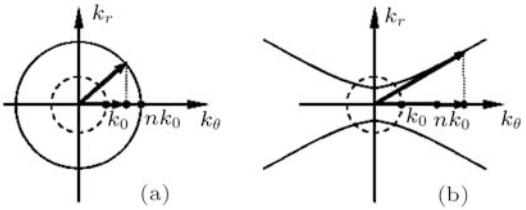


Fig. 1. Dispersion relations for (a) isotropic medium and (b) a metamaterial with $\varepsilon_r < 0$, $\varepsilon_\theta > 0$. Note that for an ordinary solid immersion lens with constant refractive index n, the maximum wave vector for propagation modes is nk_0, however, for a hyperlens, the wave vector k can take an arbitrarily large value in the metamaterial medium.

In our design, a focusing objective is employed first to transform the incident plane wave into a convergent one. Without the objective, the hyperlens should be large enough to cover all the incident plane waves, which requires more layers and then depresses the system transmission and increases the difficulty in fabrication. When the focusing objective is inserted, a smaller hyperlens can cover all the focused waves. The inserted objective can bring another benefit to the beam focusing device. According to the analysis in Ref. [15], all incident light beams on the hyperlens will travel toward the cylindrical core; however, the marginal rays ejected from the outmost layer of the

hyperlens will undergo large incident angles at the medium boundary, which will cause a large Fresnel reflection loss. Fortunately, the inserted objective ensures that each incident beam on the hyperlens arrives at normal incidence. Figure 2 shows the schematic diagram of the proposed hyperlens-based focusing device. It can be seen from Fig. 2 that the focusing device consists of two parts: one is the conventional objective and the other one is the hyperlens. The hyperlens is utilized to gradually amplify the wavenumber of the focused cylindrical wave as the wave propagates toward the inner layer of the hyperlens. Finally, the wave with a tangential wavenumber larger than k_0 for super-resolution focusing will be formed in the focal plane of the objective. Since the cylindrical shape of each layer of the hyperlens matches well with the wavefront of the convergent wave, only wavenumbers increase as the convergent wave propagates, no perturbation is presented in the wavefront, and thus the focal plane of the hybrid device will coincide with that of the focusing objective.

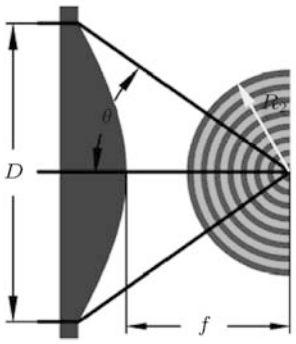


Fig. 2. Schematic diagram of the proposed hyperlens-based focusing device. The device is composed of a focusing objective and a hyperlens. The f is the focal length.

2.2. Parameter analysis

The resolution (focused spot size) and the transmission of the system are two important characteristics of the proposed beam focusing device. The resolution is related to the wavenumber. We now analyse the delivery of the wavenumber in each part of the device. Suppose that the clear aperture of the focusing objective is D, the beam size of the incident plane wave is equal to D, and the corresponding bandwidth of the angular spectrum of the incident wave is $2\pi/D$. Limited by the nature of the isotropic medium and the numerical aperture of the focusing objective, the largest transverse wavenumber of the propagating wave is nk_0. In our case, if $2\pi/D < 2nk_0$, all incident waves will be in the propagation modes and can pass through the focusing objective without a sharp decay. After the beams propagate through the focusing objective, limited by the finite value of numerical aperture N_A of the focusing objective, the largest transverse wavenumber of the propagating wave is $k_0 \sin\theta$, leading to $2\pi/(2k_0 \sin\theta) = \lambda_0/(2N_\mathrm{A})$ for the final size of the focused spot, which corresponds to the resolution limited by the diffraction. In contrast, by adding the hyperlens, waves with transverse wavenumbers exceeding k_0 will still be in propagation modes and keep focusing until they eventually reach the focal plane. The largest transverse wavenumber is proportional to $(R_2/R_1)k_0 \sin\theta$, where R_1 and R_2 are the radii of the outmost and the innermost layers of the hyperlens, respectively, and the corresponding resolution is proportional to $\lambda_0/[(R_2/R_1)\sin\theta]$.

The second important characteristic, i.e., the transmission, is influenced mainly by the intrinsic loss of the metal, which is unavoidable.[7,21–23] However, the hyperlens can be designed to optimize the filling ratio of the metal layers, resulting in a higher transmission. This can be explained by examining effective tangential dielectric permittivity $\varepsilon_\theta = p\varepsilon_\mathrm{m} + (1-p)\varepsilon_\mathrm{d}$ and radial dielectric permittivity $\varepsilon_r = \varepsilon_m\varepsilon_\mathrm{d}/[p\varepsilon_\mathrm{d} + (1-p)\varepsilon_\mathrm{m}]$, where p denotes the metal filling factor.[17] Due to the dispersion relation $k_r^2/\varepsilon_\theta + k_\theta^2/\varepsilon_r = k_0^2$ described in Section 1, $\mathrm{Im}[\varepsilon_\theta]$ and $\mathrm{Im}[\varepsilon_r]$ influence radial wave vector k_r, and the imaginary part of k_r implies the amplitude decay of the convergent wave. We simulate the $\mathrm{Im}[k_r]$ versus p with k_θ varying from k_0 to $6k_0$. The results are shown in Fig. 3. It can be seen from Fig. 3 that when p is around 0.5 for different values of k_θ, the minimum $\mathrm{Im}[k_r]$ can be obtained.

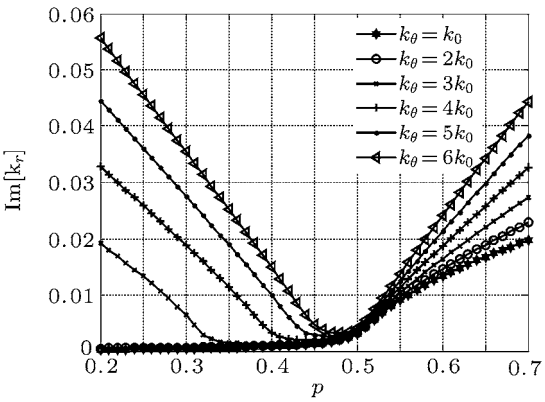


Fig. 3. The $\mathrm{Im}[k_r]$ versus p with k_θ varying from k_0 to $6k_0$. In the simulation, the dielectric material is the aluminum oxide with $\varepsilon_\mathrm{d} = 3.21$,[14] and the metal is silver with $\varepsilon_\mathrm{m} = -3.12 + 0.21\,\mathrm{i}$.[14] The working wavelength is 375 nm.

The bulk silver is chosen as the metal layer mate-

rial, because it can cause less loss than the ultra-thin silver film that has a relatively large imaginary part $\mathrm{Im}[\varepsilon_\mathrm{m}]$ of its permittivity.[22] Besides, permittivity ε_m will not remain a constant, as it becomes a function of the layer thickness[21,22] for the ultra-thin silver film.

In addition to the optimal layer thickness, the outmost layer with a small radius is also needed to achieve a high transmission system with less metal loss. However, taking the resolution into consideration, the radius of the outmost layer of the hyperlens should be large enough to deliver all waves from the focusing objective. Since the outermost layer of the hyperlens is in contact with air in our design, the maximum transverse wavenumber in air should be less than $k_0 \sin\theta$ for the propagating waves, corresponding to a minimum spots size of $\Delta x_\mathrm{min} = 2\pi/(2k_0 \sin\theta)$. Consequently, the minimum radius of the outermost layer of the hyperlens should satisfy $R_{2,\mathrm{min}} = (\Delta x_\mathrm{min}/2)/\tan\theta = \lambda_0/(4\tan\theta\sin\theta)$.

It should be noted that in the application of the optical data storage, the focused laser beam will be reflected backwards after it has reached the optical disk. The large wave vectors of the reflected beams are demagnified by the hyperlens and then gradually reduced to values less than $k_0 \sin\theta$. Following the collimation by the focusing objective and the detection by using a photodetector, the data reading process of an optical disk signal can be realized.

The fabrication of the hyperlens can follow the method mentioned in Ref. [17], while the objective lens can be fabricated by using the traditional lens fabrication procedure. And the microlens as the objective to be discussed in Section 3 can be fabricated by using the microoptics fabrication technology mentioned in Refs. [24]–[26].

3. Numerical simulations and discussion

To verify our design, a commercial finite element method program COMSOL Multiphysics$^{\mathrm{TM}}$ 3.5 was used to simulate the performance of the proposed hyperlens-based beam focusing device. The power flows in the simulation domain are shown in Fig. 4 for the focusing objective, the single half cylindrical hyperlens, and the focusing objective with a half cylindrical hyperlens respectively. For simulations shown in Figs. 4(a) and 4(c), an equal microlens is used as the focusing objective, and its main parameters are as follows. The diameter is 1.2 μm, the focal length is 0.8 μm, the numerical aperture is 0.6, and the curvature radius and the conic coefficient of the plano-convex structure are 0.5912 μm and −2.886, respectively. The material of the microlens is photoresist and has a refractive index of 1.699. For the hyperlens shown in Figs. 4(b) and 4(c), we fill the innermost hollow cylinder with alternating layers of metal and dielectric materials to lengthen the propagation distances of waves with large wavenumbers, thereby improving the focusing resolution. The parameters of the single half cylindrical hyperlens shown in Fig. 4(b) are as follows. The outmost radius is 600 nm, the layer thickness is 10 nm, and the layers are composed of alternating aluminum oxide (Al_2O_3) ($\varepsilon_\mathrm{d} = 3.21$[14]) and silver (Ag) ($\varepsilon_\mathrm{m} = -3.12 + 0.21\,\mathrm{i}$[14]). The layer materials and the thickness of the half cylindrical hyperlens shown in Fig. 4(c) are the same as those of the hyperlens shown in Fig. 4(b) except that the outmost radius is 240 nm and a microlens (the same as the case shown in Fig. 4(a)) is inserted.

It can be seen from Fig. 4(b) that many marginal beams cannot enter the hyperlens because of their large incident angles. In comparison, when a microlens is inserted (shown in Fig. 4(c)), the incident plane wave can be transformed into a convergent one first, and then each beam is incident on the hyperlens in the norm direction, which will improve the system transmission. What is more, compared with the case shown in Fig. 4(b), a small radius of the outmost layer of the hyperlens is required to cover the convergent waves, which will reduce the metal layers and then further improve the system transmission. We simulate the power flow distributions at the exit port of the hyperlens in the cross-section direction, and the results are shown in Fig. 4(d). Figure 4(d) shows that the focusing system without the hyperlens has a higher transmission ($\sim 75\%$) but a lower resolution, a single hyperlens has a higher resolution but a ultral-low transmission ($\sim 0.1\%$), and only the hybrid structure can obtain both a high resolution and a higher transmission ($\sim 5.3\%$).

Figure 4(d) shows that the spot size, the full width at half maximum (FWHM), in the focal plane of the single focusing objective is about 287.6 nm, corresponding to $\lambda_0/1.3$, which is close to the theoretical diffraction-limited spot size of $\lambda_0/2N_\mathrm{A} = 312.5$ nm ($\sim \lambda_0/1.2$). For the half cylindrical hyperlens based device, it can be seen from Figs. 4(b) and 4(c) that the

focused spot is remarkably localized within a smaller area limited by the innermost layer core, verifying the existence of large transverse wavenumbers. According to Fig. 4(d), the focusing size is 16.3 nm for the hybrid structure (FWHM, corresponding to $\lambda_0/23$), which is far smaller than the diffraction-limited spot size simulated in Fig. 4(a), and thus the super-resolution focusing is realized.

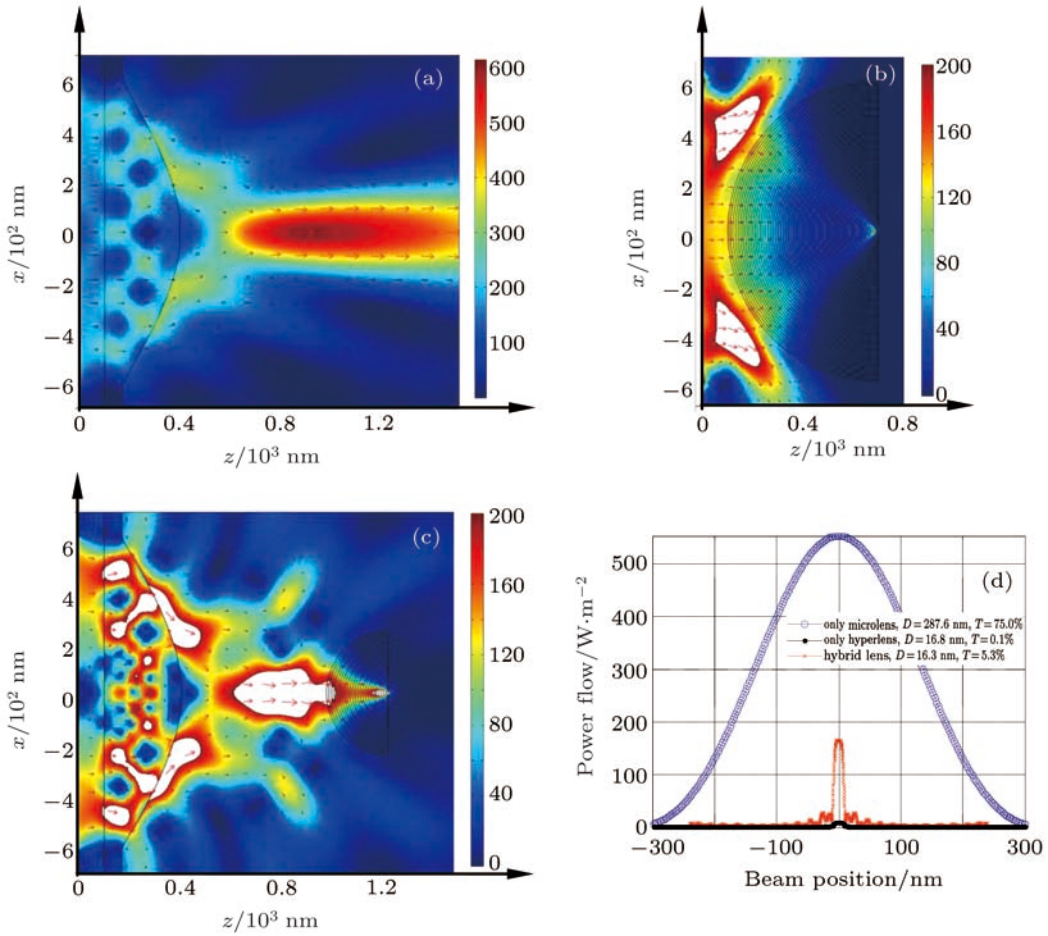


Fig. 4. (colour online) Simulations of different focusing devices with a normal incident plane wave. The working wavelength is 375 nm, and the incident wave is in the transverse magnetic mode. Panels (a), (b), and (c) show the power flow distributions in the simulation domain for a single microlens, a single hyperlens, and a microlens combining with a half cylindrical hyperlens, respectively. Panel (d) exhibits the power flow distributions in the cross-section direction of the focal plane with data taken from panels (a), (b), and (c).

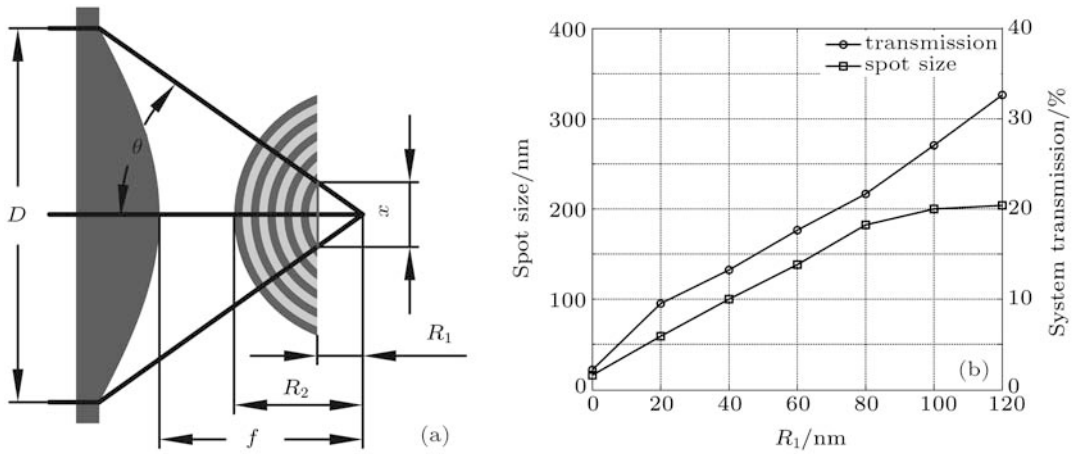


Fig. 5. (a) Schematic diagram of the modifed hyperlens-based focusing device and (b) spot size and system transmission of the device varying with innermost layer radius R_1.

In some beam focusing applications, such as the optical data storage and the photolithography, the system transmission of only 5.3% (simulated results above) is not good enough. In our optimization design, we can increase the radius of the innermost layer R_1 to reduce the layer number and thereby improve the system transmission. The schematic diagram of the modified structure is shown in Fig. 5(a). The disadvantage of the method is that the focusing spot size will increase with the increasing R_1. We calculate the spot sizes and the transmissions for different values of R_1, and the results are shown in Fig. 5(b). It can be seen from Fig. 5(b) that when R_1 increases to 120 nm, the system transmission increases to 32.6%, and the spot size increases to 203.4 nm ($\sim\lambda_0/1.8$), which is still below the diffraction limit ($\sim\lambda_0/1.2$). In applications, the structure of the device should be carefully optimized, because the focusing spot size and the system transmission are both important.

The waves with transverse wavenumbers exceeding k_0 will be in evanescent modes after passing through the hyperlens. Due to the strong diffraction and the amplitude attenuation of the waves, the spot size will increase and the system transmission will decrease when the waves leave away from the hyperlens. Therefore, the working plane should be as close to the focusing device as possible in applications.

It should be mentioned that in the optical data storage and other applications, the diameter of the collimated beam is generally much larger than 1.2 μm used in our simulation. However, as long as the numerical aperture of the focusing objective remains unchanged, the aperture and the focal length can be enlarged in proportion to the actual sizes to meet the size of the beam spot in reality without disturbing the wavefront. Then for the unchanged mode of transmission, the device proposed is still applicable.

4. Conclusion

We report a device combining a focusing objective and a hyperlens together to realize the superresolution focusing with an incident plane wave. The layout is presented for such a realization, and the device's characteristics are analysed theoretically, which is valuable for optimizing the design. The numerical simulations further verify our design and demonstrate that the minimum beam spot size can be reduced to $\lambda_0/23$ for the given focusing objective and the system transmission can exceed 5.3%. The proposed device, owing to its simple design and the realizable structure, is expected to be useful in the fields of optical data storage, nanolithography, nanofabrication, and so on.

References

[1] Durant S, Liu Z W, Steele J M and Zhang X 2006 *J. Opt. Soc. Am.* B **23** 2383

[2] Pendry J B 2000 *Phys. Rev. Lett.* **85** 3966

[3] Fang N, Lee H, Sun C and Zhang X 2005 *Science* **308** 534

[4] Melville D O S and Blaikie R J 2005 *Opt. Express* **13** 2127

[5] Liu Z W, Fang N, Yen T J and Zhang X 2003 *Appl. Phys. Lett.* **83** 5184

[6] Fang N, Liu Z W, Yen T J and Zhang X 2003 *Opt. Express* **11** 682

[7] Lee H, Xiong Y, Fang N, Srituravanich W, Ambati M, Sun C and Zhang X 2005 *New J. Phys.* **7** 1

[8] Liu Z W, Durant S, Lee H, Pikus Y, Fang N, Xiong Y, Sun C and Zhang X 2007 *Nano Lett.* **7** 403

[9] Liu Z W, Durant S, Lee H, Pikus Y, Xiong Y, Sun C and Zhang X 2007 *Opt. Express* **15** 6947

[10] Lee H, Liu Z W, Xiong Y, Sun C and Zhang X 2008 *Solid State Commun.* **146** 202

[11] Chen J, Wang Q K and Li H H 2010 *Chin. Phys.* B **19** 034202

[12] Jacob Z, Alekseyev L V and Narimanov E 2006 *Opt. Express* **14** 8247

[13] Liu Z W, Lee H, Xiong Y, Sun C and Zhang X 2007 *Science* **315** 1686

[14] Xiong Y, Liu Z W and Zhang X 2009 *Appl. Phys. Lett.* **94** 203108

[15] Jacob Z, Alekseyev L V and Narimanov E 2007 *J. Opt. Soc. Am.* A **24** 52

[16] Hu J G, Cao Y, Wang P, Lu Y H and Ming H 2008 *Chin. Phys. Lett.* **25** 4151

[17] Lee H, Liu Z W, Xiong Y, Sun C and Zhang X 2007 *Opt. Express* **15** 15886

[18] Milster T D, Jo J S and Hirota K 1999 *Appl. Opt.* **38** 5046

[19] Terris A D, Mamin H J, Rugar D, Studenmund W R and Kino G S 1994 *Appl. Phys. Lett.* **65** 388

[20] Wu Q, Feke G D, Grober R D and Ghislain L P 1999 *Appl. Phys. Lett.* **75** 4064

[21] Johnson P B and Christy R W 1972 *Phys. Rev.* B **6** 4370

[22] Chen W, Thoreson M D, Ishii S, Kildishev A V and Shalaev V M 2010 *Opt. Express* **18** 5124

[23] Smith E J, Liu Z W, Mei Y F and Schmidt O G 2009 *Appl. Phys. Lett.* **95** 083104

[24] Dong X C, Du C L, Li S H, Wang C T and Fu Y Q 2005 *Opt. Express* **13** 1353

[25] Shi L F, Du C L, Dong X C, Deng Q L and Luo X G 2007 *Appl. Opt.* **46** 8346

[26] Du C L, Dong X C, Qiu C K, Deng Q L and Zhou C X 2004 *Opt. Eng.* **43** 2595